Measurement of Interstitial Space Dispersion in Packed Bed Columns: Comparison of Superficially Porous and Fully Porous Particles

Vanderlinden, Kim; Broeckhoven, Ken; Desmet, Gert

Published in:
LC GC North America

Publication date:
2019

Document Version:
Accepted author manuscript

Measurement of Interstitial Space Dispersion in Packed Bed Columns: Comparison of Superficially porous and Fully-porous Particles

Kim Vanderlinden, Ken Broeckhoven, and Gert Desmet*

Department of Chemical Engineering, Vrije Universiteit Brussel, Brussels, Belgium

* Corresponding author: gedesmet@vub.be, tel.: +32 2 629 32 51

Keywords

Eddy dispersion
Packing quality
Longitudinal diffusion
Total pore blocking
Superficially porous particles

Abstract
The difference in packing quality of superficially porous and fully-porous columns has been measured using the total pore blocking technique. This technique physically eliminates all mass transfer band broadening contributions and hence provides the purest possible measure of the packing quality of a column. The measurements confirm earlier assertions made in literature about the generally better packing quality of superficially porous columns over fully-porous particle based columns.

1. Introduction

Producing reduced plate height curve minima that are typically on the order of 0.5 units lower than possible with fully-porous (FP) particles, the (re-)introduction of superficially porous (SP) particles around the year 2007 has absolutely revolutionized the efficiency of HPLC columns [1-6]. Part of this higher efficiency (roughly some 40 to 50%) can be attributed to the fact that SP particles exhibit a lower longitudinal diffusion band broadening (presence of core partially blocks the longitudinal diffusion and most SP particles have a lower internal porosity which also tends to slow down diffusion) as well as a lower stationary phase mass transfer resistance (presence of core minimizes internal diffusion distances). The latter however typically accounts for some 5 to 10% of the observed gain, which is considerably smaller than claimed in the advertisements of some superficially porous particle manufacturers.

The remaining 40 to 55% of the gain hence necessarily needs to be attributed to the fact that superficially porous columns display a significantly lower eddy-dispersion (so-called A-term band broadening describing the packing heterogeneity). The reason underlying this *a priori* unexpected effect is a problem that has not been fully resolved up to now. There have been speculations on differences in surface roughness leading to differences in packing quality [3]. Another proposed explanation was that SP particles have a markedly narrower particle size distribution than FP particles, which can in turn be expected to lead to more uniform packings. This explanation has however also been the subject of considerable controversy [3,7,8]. Nevertheless, the fact that the introduction of FP particles with a narrower PSD also lead to a marked decrease in h-values has now recently brought new evidence to support this hypothesis [9].

Traditionally, the eddy-dispersion is determined by subtracting known (or estimated values) of the longitudinal diffusion and the mobile and stationary phase mass transfer resistances (so-called C_m- and C_s-term, see Eqs. 2 and 3 further on) from the measured plate height. However, the model for the mobile phase mass transfer resistance is still under debate and the observed eddy-dispersion plate heights tend to depend on the retention factor and the intra-particle dispersion of the analytes, complicating the direct comparison of superficially porous and fully-porous columns.

In the present contribution, the mass transfer resistance contributions are physically switched off using the so-called total pore blocking (TPB)-technique to render the mesoporous space of the particles

completely inaccessible for the injected analytes [10,11]. As a consequence, the mass transfer processes are blocked and the only remaining source of band broadening (apart from the longitudinal diffusion) is the heterogeneity of the interstitial space.

In brief, the TPB-method works as follows. First, the column is flushed with a solvent such as isopropanol (IPA) that is fully miscible with both hydrophobic and hydrophilic liquids. Subsequently the column is filled with a strong hydrophobic solvent, e.g., decane, which can fully replace the IPA in both the interstitial space as well as in the particle meso-pores (Fig. 1a). Next, the decane is pushed out of the interstitial space again using a hydrophilic buffer that is immiscible with the decane. Due to the high affinity of the decane for the C_{18} layer inside the mesopores, the decane cannot be removed from the particle's interior (Fig. 1b). Injecting now a strongly hydrophilic marker (e.g., potassium iodide, KI), this marker will not be able to penetrate the particles, mimicking (at least for the marker) a completely non porous column.

The TPB-technique was originally introduced to make accurate measurements of the external porosity (ε) of packed columns [10,11]. Conventionally this is measured using so-called inverse size exclusion chromatography (ISEC). Whereas the polystyrene standards used in ISEC have difficulties to access the smallest spaces of the interstitial volume and thus require an extrapolation to assess the full extent of the interstitial space, the TPB-method works with small molecule tracers that can explore the entire space.

Since its introduction, TPB has been used frequently by others [9,12-16]. Here, we report on the TPB-measurement to investigate differences in interstitial space dispersion between FP and SP particles. This was done on a set of 4.6x150mm columns packed with 5μm particles. These dimensions were purposely selected to minimize contributions from extra-column sources, because the peaks under TPB conditions elute at zero retention (as a matter of fact they even elute before the t_0-marker of the unblocked column) and are hence very narrow.

2. Experimental

All experimental work was performed on an Agilent 1290 Infinity UHPLC system with a 1260 DAD equipped with an 80 or 500nL detector cell (Agilent Technologies, Waldbronn). All columns used in this study were 4.6x150mm columns, packed with either FP or SP with a diameter of 5μm and C_{18}-derivatized. Excel (FP_A) and Ultracore (SP_A) columns from ACE as well as Luna (FP_B) and Kinetex (SP_B) columns from Phenomenex were compared. van Deemter measurements on the unblocked columns were performed at flowrates ranging from 0.05 to 2mL/min with a mobile phase of 50v/v% (Ultracore) or 49v/v% (Excel) acetonitrile (ACN, Biosolve B.V.) in water, to obtain the same retention factor for butyrophenone. A mixture of KI, acetophenone, propiophenone and butyrophenone (Sigma-Aldrich), all dissolved to a concentration of 100μg/mL in the mobile phase solvent, was used as the sample to study the column under retained (=open-pore) conditions. In order to block the columns, they were flushed with IPA (Biosolve B.V.) at a flowrate of 0.2mL/min for 60min, subsequently filled with decane (Acros organics) at a flowrate of 0.2mL/min for approximately 100 column volumes and finally flushed with a 10mM ammonium acetate (Sigma-Aldrich) buffer (pH=3) at a flowrate of 0.4mL/min [10]. Retention times under blocked pore conditions were measured by injecting 500μg/mL of KI dissolved in the buffer every 5min during this final flushing step. The same buffer and KI sample were used to measure the van Deemter curves on the blocked columns. All measurements were performed at 30°C, at a wavelength of 254nm and a frequency of 40Hz and the injection volume was set to 1μL. Peak widths were measured at half height and 4.4% height (5σ).

Reduced van Deemter plots were calculated using the nominal value of the particle size as mentioned by the manufacturer ($h=H/d_p$). Based on the experimentally measured permeability and porosity of the different columns, the SP and FP columns of the same vendor had a difference in particle size less than 3% and varied at the most 10% from their nominal size. Since only a relative comparison of column performance between columns of the same vendors are discussed, the true value of the particle has no impact on the conclusions. For the the diffusion coefficients, experimentally measured values reported in [17] were used, for the given component and employed mobile phase composition ($\nu_i = u_i \cdot d_p/D_m$), with D_m equal to 1.2 10^{-9} m^2/s for acetophenone and 2.1 10^{-9} m^2/s for KI.

3. Results and discussion

3.1 Unblocked pore dispersion

First the columns were tested under retained component conditions, i.e., with normally accessible meso-pores. The resulting reduced van Deemter curves for acetophenone are shown in Fig. 2a. The curves display the typically observed difference between both particle types: whereas the fully-porous column produces a minimal reduced plate height of h_{min}=2.1 (indicative a well-packed column [18]), the superficially porous column produces a significantly lower minimum (h_{min}=1.2). These minima are obtained at an optimal velocity around ν_{opt}=9 for both the fully-porous and the superficially porous column. A similar difference (on the order of 0.8 to 1 reduced plate height units) is observed for the other, more strongly retained test analytes (data not shown). For the stronger retained compounds the absolute h_{min}-values are also shifted to a larger value because of the larger B-term contribution typically observed for components with at higher k. For the same reason, the optimal velocity is shifted to a somewhat larger value with increasing retention.

The data were fitted using the free-exponent Knox-model [19], producing a good fit (R^2=0.98-0.999):

$$h = A\nu_i^n + B/\nu_i + C\nu_i \quad (1)$$

This model has been preferred over the more frequently used fixed-exponent Knox-model (where n is fixed at n=0.333). The original data set on which the classic n=0.333-value was based was rather limited, while later work showed the exponent itself contains relevant information on the packing and can vary considerably (cf. range between n=0.5 and n=1 in [19]). The resulting fitting parameters are given in Table 1. During the fitting, the C-term constant was fixed at the C_s-constant value found from Eq. (2) discussed further on. In agreement with its larger overall h-values, the A-, B-, and C-term constants of the FP column are clearly higher than those found for the SP column. The n-exponent (order of n=0.45 to n=0.5) is typical for the behavior of a retained analyte in a packed bed column [19].

Fig. 2b shows what remains of the observed band broadening when subtracting the contribution of the longitudinal diffusion. Because of the subtraction, all curves now tend to zero when ν_i tends to zero. As can be noted, the difference between the SP and the FP column is about 0.57 reduced plate height units at the ν_i=9 (h-minimum of the two particle types in Fig. 2a). This shows that roughly 35% of the difference between the fully-porous and the superficially porous column can be attributed to the difference in B-term. As explained in [20-22], the significantly lower B-term band broadening of superficially porous

particles is due to both the presence of the core as well as to the fact that the fabrication processes of the majority of the vendors leads to a mesoporous shell layer with a relatively low internal porosity.

Using the fitted value of the B-term to deduce the diffusion coefficient (D_{pz}) inside the mesoporous zone of the particles using the effective medium theory [20], we respectively obtained a value of D_{pz}=7.8 10^{-10} m^2/s (fully-porous) and D_{pz}=4.2 10^{-10} m^2/s (superficially porous). These values indicate the true transport rate inside the mesoporous material of the superficially porous particles is significantly smaller (close to a factor 2) than in the fully-porous particles. This has been observed in the past as well [20, 23] and has been explained there by differences in synthesis procedures and a concomitant difference in internal porosity. With these values, we can now calculate the expected contribution of the intra-particle mass transfer resistance (h_{Cs}) (so-called C_s-term band broadening):

$$h_{Cs} = \frac{2}{\alpha}\frac{1}{Sh_{part}}\frac{k''}{(1+k'')^2}\frac{D_m}{D_{pz}}\nu_i \qquad (2)$$

With α, the shape factor, equal to 6 for packed bed spheres, k'' the zone retention factor (k''=(1+k')($\varepsilon_T/\varepsilon$)-1), ε and ε_T the external and total porosity respectively and Sh_{part} given by Eq. (T-35) in Andrés et al. [24].

From Eq. (2), it can be calculated that the difference in h_{Cs} around the optimal velocities (ν_i=9) is only on the order of about 0.025 reduced plate height units. I.e., only about 3% of the difference in h_{min} observed in Fig. 2a can be attributed to the presence of the core. Obviously, this effect is much smaller than the initial claims made by some manufacturers.

A similar exercise can be made to estimate the expected mobile zone mass transfer resistance (h_{Cm}) (so-called C_m-term band broadening):

$$h_{Cm} = \frac{2}{\alpha}\frac{1}{Sh_m}\frac{k''^2}{(1+k'')^2}\frac{\varepsilon}{1-\varepsilon}\nu_i \qquad (3)$$

with Sh_m given by Eq. 11 in Deridder et al. [25]. With the known k''-value(s), and using α=6 for spherical particles and the ε-values determined below (see discussion of Fig. 3) it can be calculated that the difference in h_{Cm} around ν_i=9 is on the order of about 0.02 reduced plate height units, corresponding to some 2% of the difference observed in Fig. 2a.

3.2 Blocked pore dispersion

The above analysis implies the remaining difference must be due to differences in eddy-dispersion, i.e., due to differences in packing quality and interstitial space heterogeneity. To investigate and measure this difference in the absence of any intra-particle contribution (to have the purest possible measure of the dispersion in the interstitial space), the columns were subsequently blocked following the procedure established in [10]. During the flushing step needed to make the gradual transition between condition 1 and condition 2 in Fig. 1, the relative retention volume of the KI marker ($F \cdot t_i/V_G=\varepsilon$ with V_G geometrical volume of open column) is continuously monitored until this value reaches its plateau value (see Fig. 3 for example). Reaching the plateau is indicative of the state (Fig. 1b) wherein the interstitial space is

completely cleared of the decane originally occupying it (Fig. 1a). This event is typically also marked by the fact that the detector trace becomes flat and stable again, after a period of strong disturbances caused by small amounts of decane passing the detector.

A final control to verify whether the entire interstitial space is cleared of decane is made by verifying that the pressure needed to send a given flow rate F through the column in the blocked state is equal to that required in the unblocked state. If this is the case, it can be guaranteed the interstitial space is in both cases the same [10]. This can be understood by writing the well-known Kozeny-Carman equation in the following form [26], showing that for a given F the measured pressure drop only depends on the external porosity and is independent of the intra-particle porosity:

$$\Delta P = \frac{180}{d_p^2}\frac{(1-\varepsilon)^2}{\varepsilon^2}\frac{F}{A\cdot\varepsilon}\mu\cdot L \tag{4}$$

wherein d_p is the particle diameter, ε the external porosity, F the flowrate, A the cross-sectional area, μ the viscosity and L the column length.

If part of the interstitial space would still be occupied by a remaining fraction of decane, these would reduce the accessible interstitial space, and the mobile phase flow would experience a smaller external porosity ε. As can be noted from Eq. (4), showing a strong dependency between ΔP and ε (close to a ε^{-5}-dependency), even a small decrease in ε can already be expected to lead to a significant increase of the required inlet pressure. Fig. 4 shows one of the pressure tests conducted in the plateau phase of Fig. 3 to verify this. As can be noted, the measured pressures before and after blocking the column all lie close to the bisecting line, thus indicating the above criterion is satisfied and indicating the interstitial space under blocked conditions is indeed identical to the actual interstitial space observed in the open-pore conditions.

Fig. 5 shows some of the KI tracer peaks eluting from the column in the plateau phase, i.e., under perfect blocking conditions. The peaks eluting from the FP column are clearly broader than those eluting from the SP column over the entire range of different flow rates, indicating the former suffers from a significantly larger packing heterogeneity than the latter. The difference also clearly increases with increasing flow rate. This is mainly due to the fact that, at the lower flow rates, a significant part of the band broadening is due to longitudinal diffusion which is to a very large extent is independent of the degree of packing heterogeneity (see also small differences between B-term values in Table 1).

The observations in Fig. 5 are more quantitatively and comprehensively represented in the reduced van Deemter plots (h_{TPB} versus ν_i) in Fig. 6. These show a clear difference (of around 0.2 to 0.3 reduced plate height units) between the fully-porous and the superficially porous column also shown in Fig. 2. The contribution of the extra-column dispersion can be estimated to be on the order of $5\mu L^2$, i.e., about 5% at $\nu_i=\nu_{opt}$ and around 8% at the highest ν_i. For low ν_I the curves appears to cross, but this should not be emphasized too much as it was recently shown that even small errors of the values for the B-term result in large deviations in the estimated h-h_B values at low velocity (ν_I<2) [27].

An important observation from Fig. 6 is that the h_{TPB}-values are of the same order (and even larger in the superficially porous case) than the h-values observed in Fig. 2a. This implies the dispersion measured using the total pore blocking technique cannot simply be considered as a measurement of the eddy-dispersion

contribution prevailing under normal open-pore conditions, i.e., it cannot be seen as a measurement of the first term of Eq. (1). This lack of correspondence is due to the fact that the total pore blocking technique is measuring the dispersion under different boundary conditions at the particle outer surface than in the open-pore case (no diffusion towards and through the particles in blocked pore case, equal diffusion fluxes and chemical potentials in the open-pore case). However, this does not imply the measured differences under total pore blocking conditions, are not relevant. On the contrary, it is precisely the absence of any interference with the intra-particle and trans-particle diffusion that makes the h_{TPB}-values the purest possible measurement of the packing homogeneity of a column.

The same comparison was also conducted for another set of FS and SP particle columns from a different vendor. In this case, two columns were tested per particle type and the curves represented in Fig. 7 show the average of the two columns.

The h_{TPB}-curves in Figs. 7 have also been fitted with Eq. (1). This was done by keeping the C-term constant at C=0 to represent the absence of any mass transfer to and in the particles. One interesting observation from the fitting parameters shown in Table 1 is that the difference between the B-term constants of the SP and FP particles has dropped below the significance level. This is again in agreement with the fact that longitudinal diffusion is known to be virtually independent of the packing heterogeneity. The actual B-values are somewhat smaller than the theoretically expected value around 1.5 but this can be attributed to the lack of a sufficient number of data points in the low ν_i-range. Another observation from Table 1 is that the n-values are significantly smaller in the blocked pore conditions than in the open pore conditions. A lower n indicates a larger contribution of velocity biases that are terminated by changes in the velocity field compared to those terminated by lateral diffusion. This makes perfect sense, given the blocked particles are now reducing the possibilities for trans-particle diffusion equilibration.

4. Conclusions

The total pore blocking technique can be used to measure the interstitial space dispersion in the absence of any inter-, intra- or trans-particle mass transfer contribution. Subsequently also removing the B-term contribution, the plots in Figs. 6b and 7b clearly show that fully-porous particle columns tend to have a higher interstitial space dispersion (i.e., packing heterogeneity) than superficially porous particle columns. This was confirmed for two different vendors. The difference in dispersion, expressed in reduced plate height units, increases with increasing velocity. Around the minimum of the retained component van Deemter curve (ν_{opt}=9), the difference is on the order of 0.6 to 0.8 reduced plate height units, depending on the column manufacturer.

Given the very small peak volumes eluting under pore blocking conditions, the measurements are limited to columns with a large volume packed with large particles. The latter is also needed to prevent high pressures that would make the blocking agent leak or contract.

Acknowledgements

The authors would like to thank Advanced Chromatography Technologies Ltd (ACE), Achrom and Phenomenex for the gift of the columns used in this study.

References

[1] S. Fekete, E. Oláh, and J. Fekete, *J. Chromatogr. A* **1228,** 57–71 (2012).
[2] R. Hayes, A. Ahmed, T. Edge, and H. Zhang, *J. Chromatogr. A* **1357,** 36–52 (2014).
[3] G. Guiochon, and F. Gritti, *J. Chromatogr. A* **1218**, 1915–1938 (2011).
[4] Y. Vanderheyden, D. Cabooter, G. Desmet, and K. Broeckhoven, *J. Chromatogr. A* **1312**, 80–86 (2013).
[5] D.V. McCalley, *J. Chromatogr. A* **1193**, 85–91 (2008).
[6] J.J. Kirkland, T.J. Langlois and J.J. DeStefano, *Am. Lab.* **39**, 18-21 (2007).
[7] D. Cabooter, A. Fanigliulo, G. Bellazzi, B. Allieri, A. Rottigni, and G. Desmet, *J. Chromatogr. A* **1217,** 70-74 (2010).
[8] F. Gritti, D.S. Bell and G. Guiochon, *J. Chromatogr. A* **1355**, 179-192 (2014).
[9] O.H.Ismail, M. Catani, L. Pasti, A. Cavazzini, A. Ciogli, C. Villani, D. Kotoni, F. Gasparrini, and D. S.Bell, *J. Chromatogr. A* **1454**, 86-92 (2016).
[10] D. Cabooter, F. Lynen, P. Sandra, and G. Desmet, *J. Chromatogr. A* **1157**, 131-141 (2007).
[11] A. Liekens, D. Cabooter, J. Denayer, and G. Desmet, *J. Chromatogr. A* **1217**, 6754-6761 (2007).
[12] N. M. Devitt, R. E. Moran, J. M. Godinho, B. M. Wagner, and M. R. Schure, *J. Chromatogr. A* **1595,** 117-126 (2019).
[13] C. Stassen, G. Desmet, K. Broeckhoven, L. Van Lokeren, and S. Eeltink, *J. Chromatogr. A* **1325**, 115-120 (2014).
[14] F. Gritti and G. Guiochon, *AIChE J.* **56**, 1495–1509 (2010).
[15] F. Gritti and G. Guiochon, *AIChE J.* **57**, 333–345 (2011).
[16] Nándor Lambert and A. Felinger, *J. Chromatogr. A* **1565,** 89-95 (2018).
[17] H. Song, Y. Vanderheyden, E. Adams, G. Desmet, and D. Cabooter, *J. Chromatogr. A* **1455,** 102–112 (2016).
[18] J.H. Knox, *J. Chromatogr. A* **831**, 3–15 (1999).
[19] J.H. Knox, *J. Chromatogr. A* **960**, 7-18 (2002).
[20] A. Liekens, J. Denayer, and G. Desmet, *J. Chromatogr. A* **1218**, 4406-4416 (2011).
[21] F. Gritti, A. Cavazzini, N. Marchetti, and G. Guiochon, *J. Chromatogr. A* **1157**, 289-303 (2007).
[22] F. Gritti, I. Leonardis, J. Abia, and G. Guiochon, *J. Chromatogr. A* **1217**, 3819-3843 (2010).
[23] F. Gritti and G. Guiochon, *Chem. Eng. Sc.* **66**, 3773-3781 (2011).
[24] A. Andrés, K. Broeckhoven, and G. Desmet, *Analytica Chimica Acta* **894**, 20-34 (2015).
[25] S. Deridder and G. Desmet, *J. Chromatogr. A* **1227**, 194-202 (2012).
[26] D. Cabooter, J. Billen, H. Terryn, F. Lynen, P. Sandra, and G. Desmet, *J. Chromatogr. A* **1178**, 108–117 (2008).
[27] H. Song, D. Sadriaj, G. Desmet and D. Cabooter, J. *Chromatogr. A* **1532**, 124-135 (2018).

Figure captions

Figure 1: Schematical representation of the total pore blocking principle showing the column composition **(a)** after the column is completely filled with decane and **(b)** after all the decane is chased out of the interstitial space by flushing the column with an immiscible, hydrophilic buffer.

Figure 2: (a) Reduced plate height plot and **(b)** B-term subtracted reduced plate height plot for acetophenone (k'=1.6) on the FP_A and SP_A columns before blocking. Curve fits according to Eq. (1). FP_A: blue dots and SP_A: red triangles.

Figure 3: Plot of the external porosity vs. time during the flushing step of the total pore blocking method of the SP_B column.

Figure 4: Plots of the measured pressures after blocking the column vs. the measured pressures before blocking of the column for the SP_A column.

Figure 5: Overlay of the chromatogram peaks for KI of the blocked columns at three different interstitial velocities **(a)** u_i = 0.25 mm/s, **(b)** u_i = 2.0 mm/s and **(c)** u_i = 3.2 mm/s. Blocked FP_B in blue and Blocked SP_B in red.

Figure 6: (a) Reduced plate height plot and **(b)** B-term subtracted reduced plate height plot for KI on the FP_A and SP_A columns after blocking. Curve fits according to Eq. (1). Blocked FP_A: blue dots and Blocked SP_A: red triangles.

Figure 7: (a) Reduced plate height plot and **(b)** B-term subtracted plate height plot for KI on the FP_B and SP_B columns after blocking. Curve fits according to Eq. (1). Blocked FP_B: blue dots and Blocked SP_B: red triangles.

Table 1: Fitted parameter values for (Eq. 1) of all columns.

Name	A	B	C*	n
FP_A	0.43	6.23	0.0094	0.48
SP_A	0.26	3.31	0.0070	0.44
Blocked FP_A	1.01	1.16	0	0.32
Blocked SP_A	1.18	1.03	0	0.14
Blocked FP_B	0.82	1.03	0	0.30
Blocked SP_B	0.58	1.24	0	0.24

* For the blocked columns the C-term was set at C=0 as mentioned in the text.

Figure 1

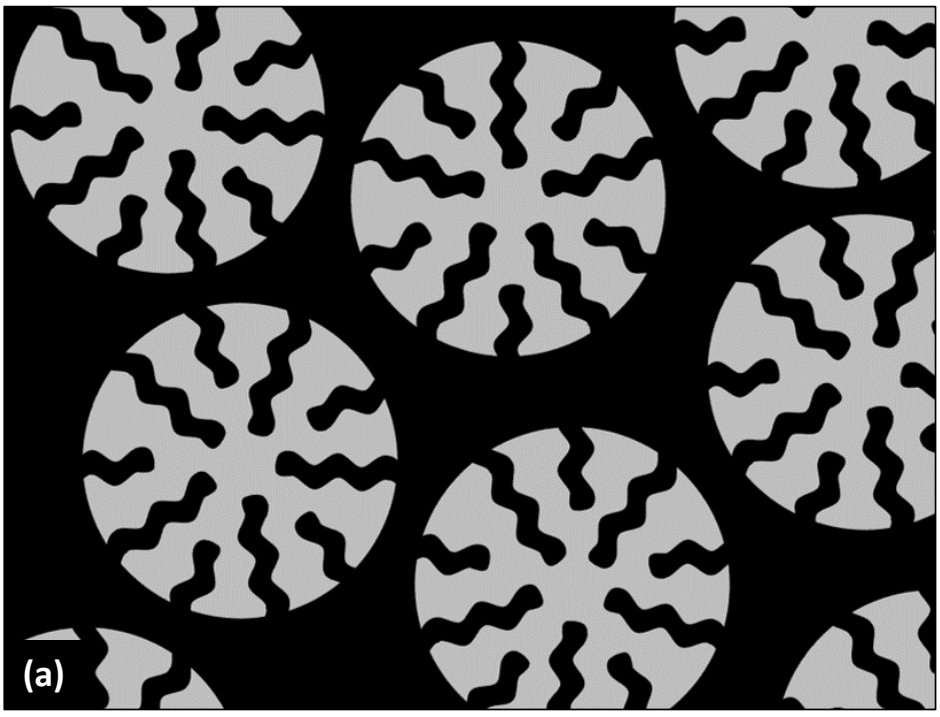
(a)

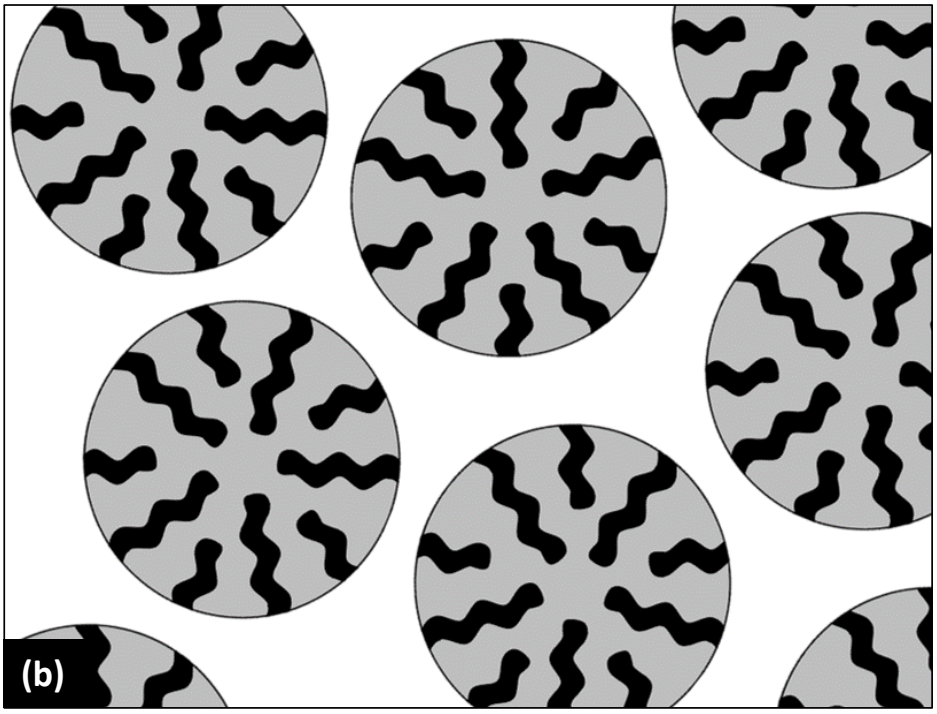
(b)

Figure 2

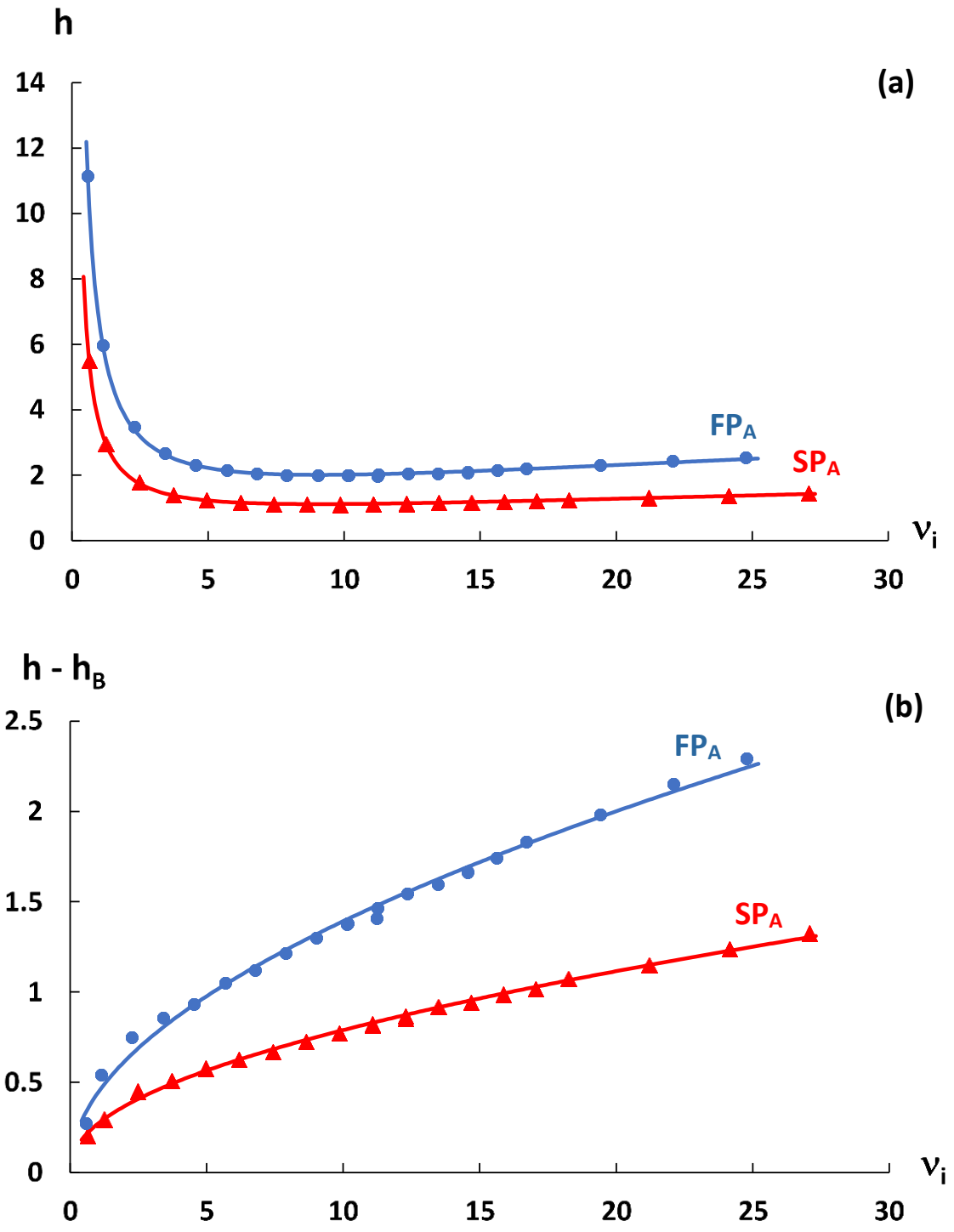
h
(a)
14
12
10
8
6
4
2
0
0
5
10
15
20
25
30
ν_i
FP_A
SP_A
h - h_B
(b)
2.5
2
1.5
1
0.5
0
0
5
10
15
20
25
30
ν_i
FP_A
SP_A

Figure 3

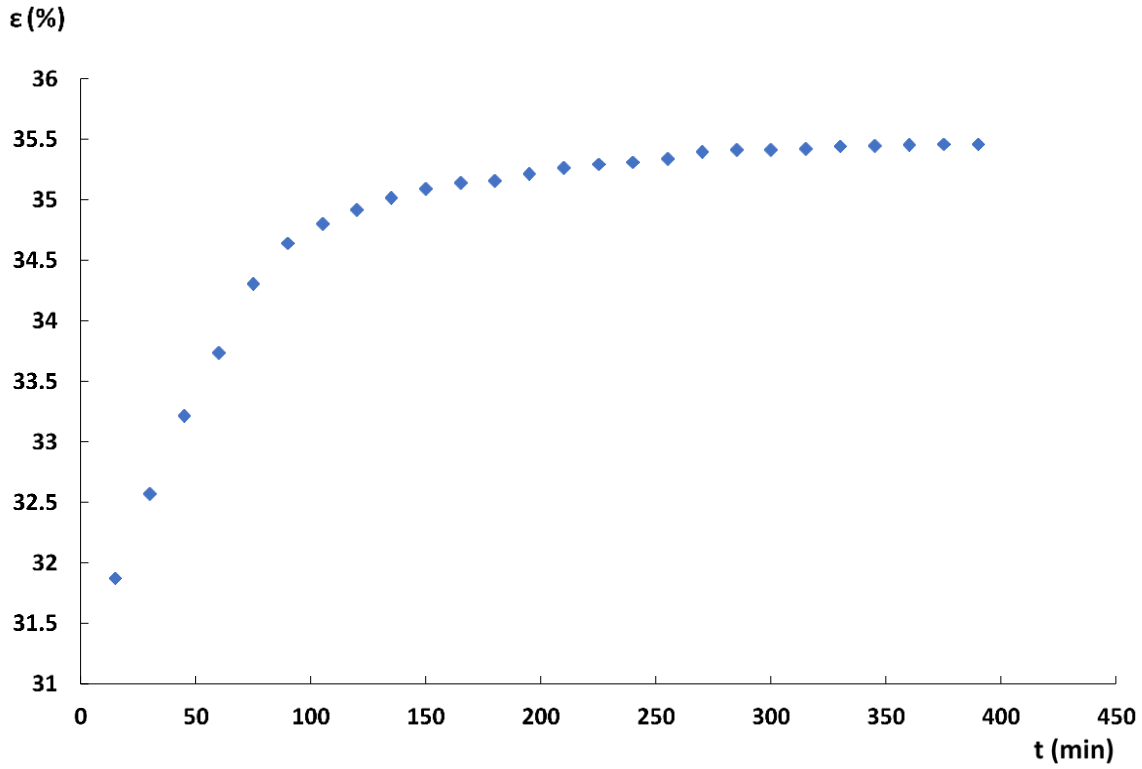
ε (%)
36
35.5
35
34.5
34
33.5
33
32.5
32
31.5
31
0
50
100
150
200
250
300
350
400
450
t (min)

Figure 4

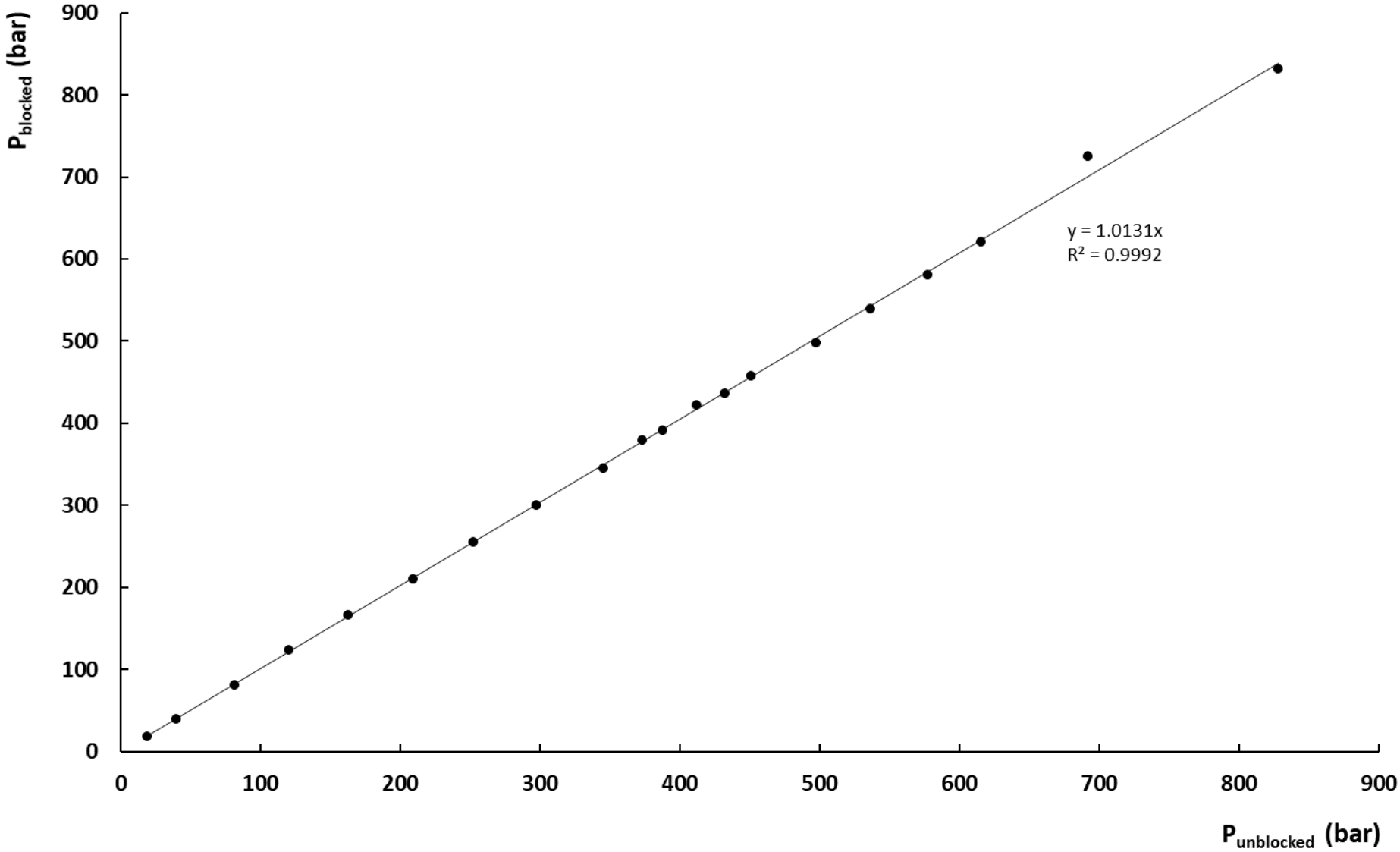
$P_{blocked}$ (bar)
900
800
700
600
500
400
300
200
100
0
0
100
200
300
400
500
600
700
800
900
$P_{unblocked}$ (bar)
y = 1.0131x
R² = 0.9992

Figure 5

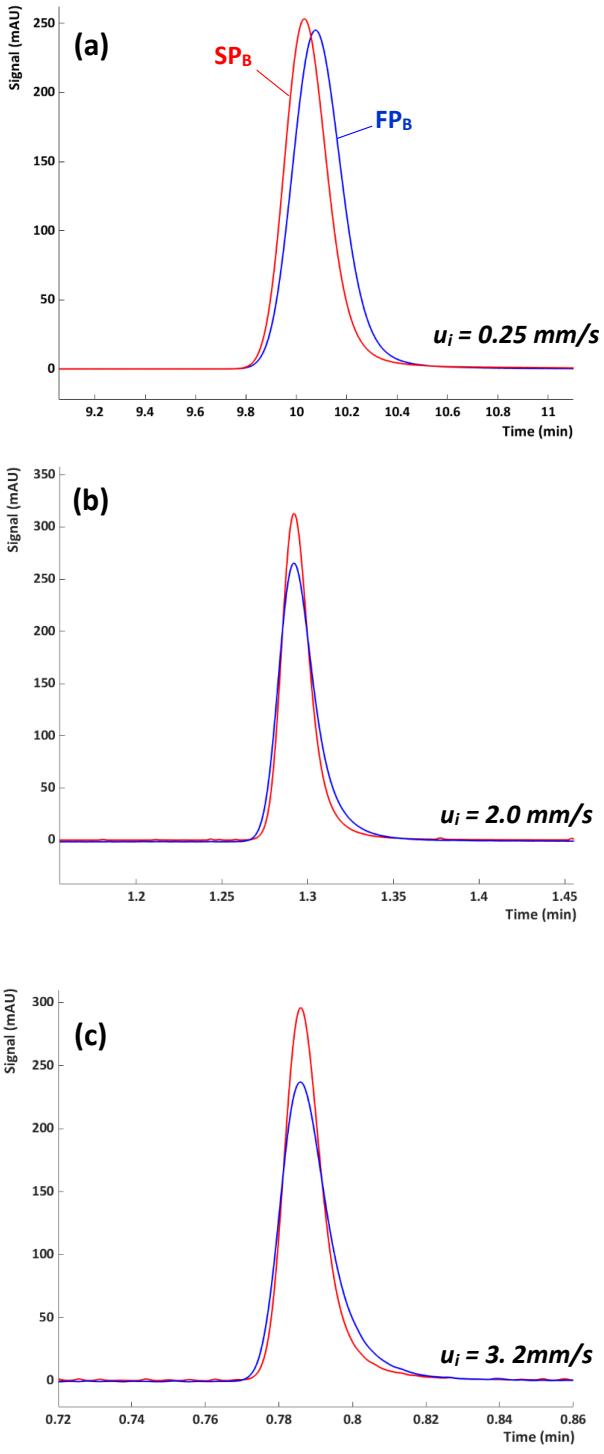

Figure 6

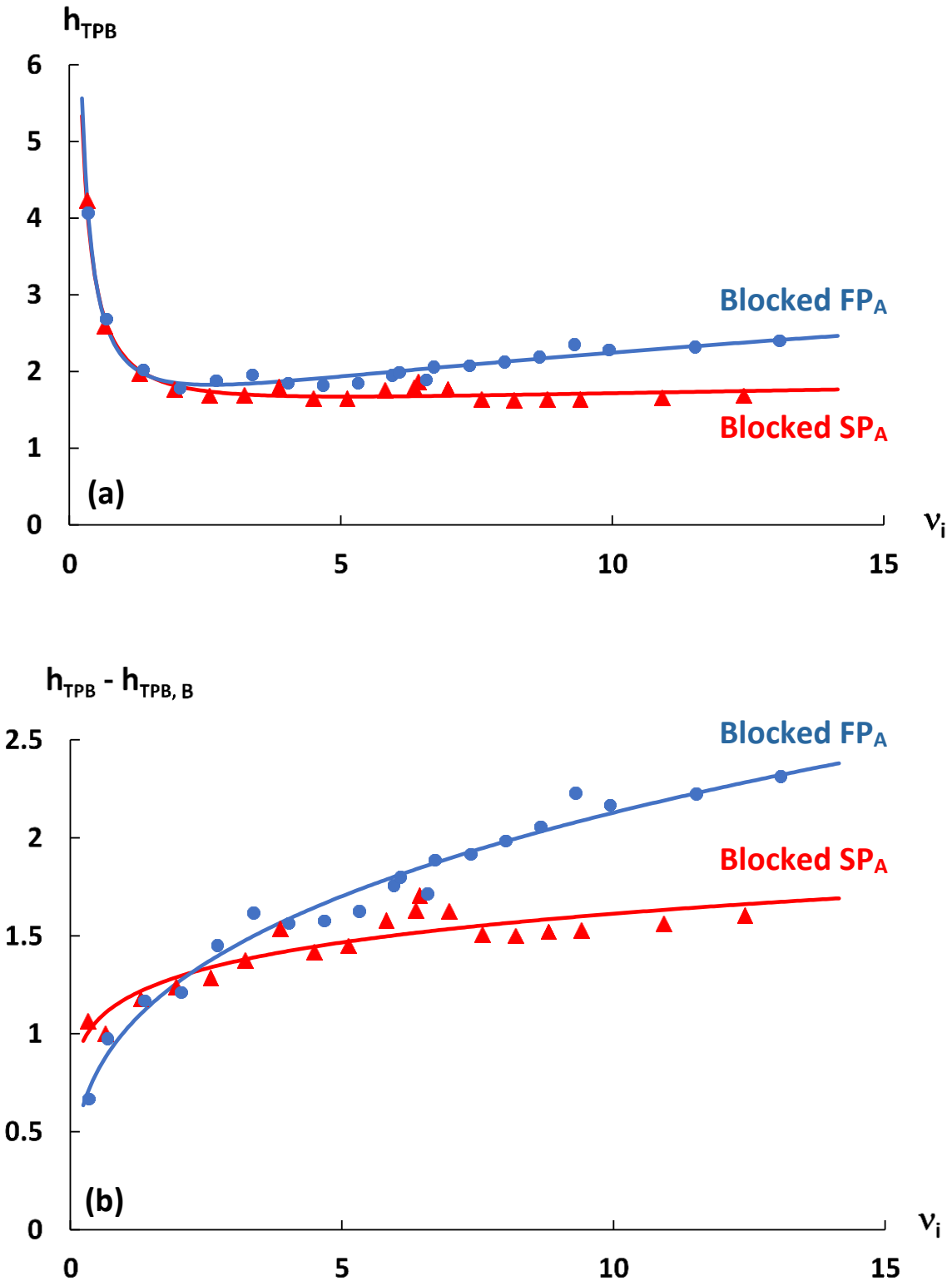
h_{TPB}
6
5
4
3
2
1
0
Blocked FP_A
Blocked SP_A
(a)
0
5
10
15
ν_i
$h_{TPB} - h_{TPB, B}$
2.5
2
1.5
1
0.5
0
Blocked FP_A
Blocked SP_A
(b)
0
5
10
15
ν_i

Figure 7

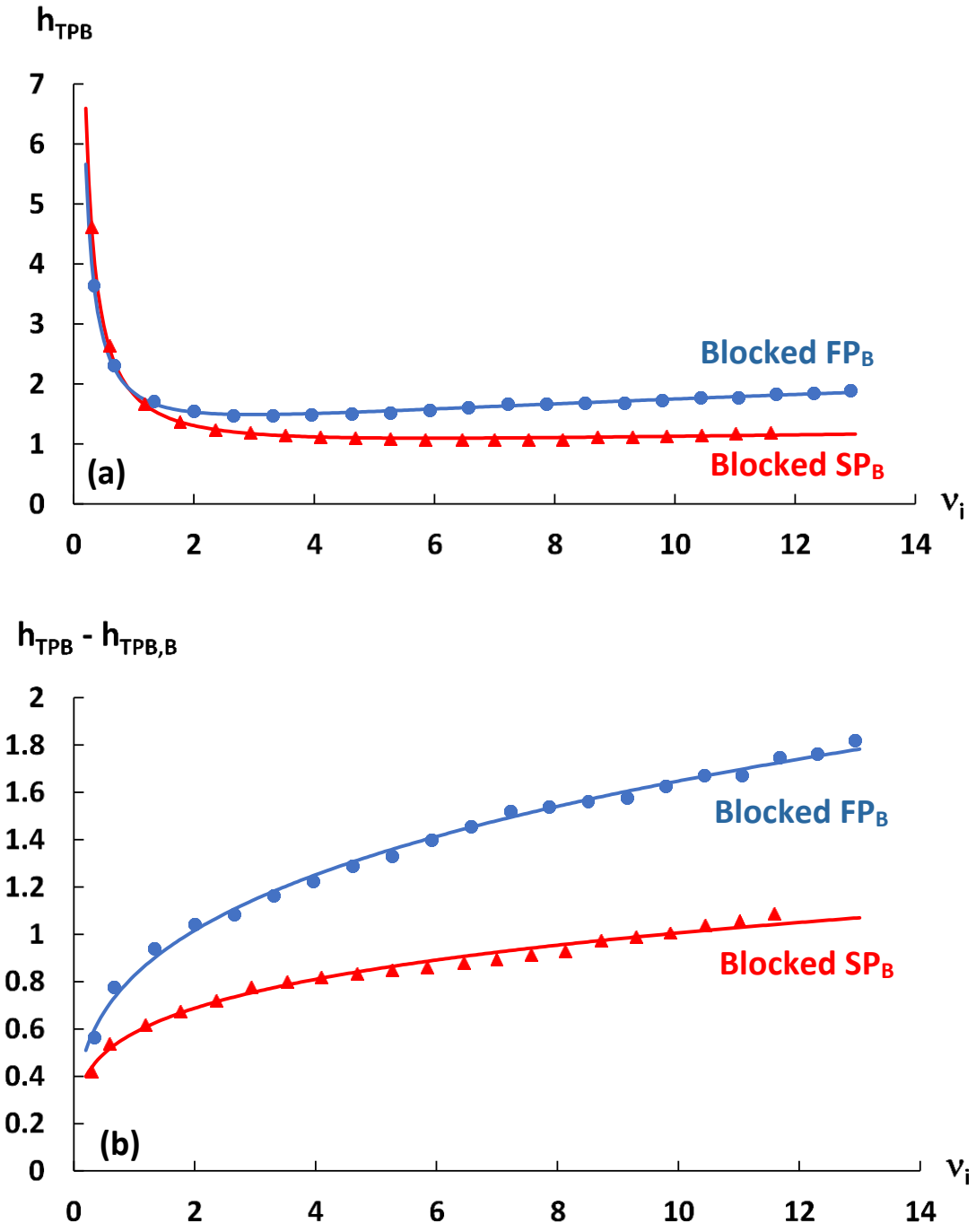
h_{TPB}
7
6
5
4
3
2
1
0
Blocked FP_B
Blocked SP_B
(a)
ν_i
0
2
4
6
8
10
12
14
$h_{TPB} - h_{TPB,B}$
2
1.8
1.6
1.4
1.2
1
0.8
0.6
0.4
0.2
0
Blocked FP_B
Blocked SP_B
(b)
ν_i
0
2
4
6
8
10
12
14